

Pomeron and Odderon Regge Trajectories from a Dynamical Holographic Model

Eduardo Folco Capossoli^{1,2,*} Danning Li^{3,†} and Henrique Boschi-Filho^{1,‡}

¹*Instituto de Física, Universidade Federal do Rio de Janeiro,
21.941-972 - Rio de Janeiro-RJ - Brazil*

²*Departamento de Física, Colégio Pedro II,
20.921-903 - Rio de Janeiro-RJ - Brazil*

³*Institute of Theoretical Physics, Chinese Academy
of Science (ITP, CAS), 100190 - Beijing - China*

Abstract

In this work we use gauge/string dualities and a dynamical model that takes into account dynamical corrections to the metric of the anti de Sitter space due to a quadratic dilaton field and calculate the masses of even and odd spin glueball states with $P = C = +1$, and $P = C = -1$, respectively. Then we construct the corresponding Regge trajectories which are associated with the pomeron for even states with $P = C = +1$, and with the odderon for odd states with $P = C = -1$. We compare our results with those coming from experimental data as well as other models.

PACS numbers: 11.25.Wx, 11.25.Tq, 12.38.Aw, 12.39.Mk

*Electronic address: educapossoli@if.ufrj.br

†Electronic address: lidn@itp.ac.cn

‡Electronic address: boschi@if.ufrj.br

I. INTRODUCTION

Quantum Chromodynamics (QCD) is a non-abelian gauge theory that describes the strong interactions between quarks and gluons. Despite the fact that gluons do not carry electric charges, they have color charge. Due to this fact, they can couple to each other and form bound states called glueballs which have not been detected so far, becoming itself a great QCD quest. At high energies the QCD coupling is small and perturbative methods work well. At low energies where bound states form (hadronization) QCD coupling is large and perturbative methods fail.

Various current studies deal with glueball issues from both experimental and theoretical points of view [1, 2]. On the theoretical side one can see several approaches such as lattice QCD, the flux tube model, MIT bag model, Coulomb Gauge model and QCD Sum Rules [1]. There is also a novel approach based on holography or AdS/CFT or Anti de Sitter/Conformal Field Theory correspondence [3–7] to circumvent the difficulty of non-perturbative QCD at low energies.

Motivated by last ten years of efforts based on AdS/CFT correspondence to investigate glueball states [8–24] the main objective of this work is to calculate the masses for both even and odd spin glueballs and obtain the Regge trajectories related to the pomeron and the odderon. We use a dynamical holographic model, taking into account dynamical corrections to the anti de Sitter (AdS) space metric due to a quadratic dilaton field. This is the first calculation of high spin glueballs ($J > 2$) with a dynamical model. This allows us to solve open some questions on the Regge trajectories for the pomeron and the odderon.

The AdS/CFT correspondence or duality is a powerful tool to tackle non-perturbative Yang-Mill theories. This duality relates a conformal Yang-Mills theory with the symmetry group $SU(N)$ for very large N and extended supersymmetry ($\mathcal{N} = 4$) with a IIB superstring theory in a curved space, known as anti de Sitter space, or $AdS_5 \times S^5$. At low energies string theory is represented by an effective supergravity theory, due to this reason the AdS/CFT is also known by gauge/gravity duality.

After breaking the conformal symmetry one can build phenomenological models that describe approximately QCD. These models are known as AdS/QCD models.

In order to deal with conformal symmetry breaking the works [8–11] have done some important progress with this issue. In these works, emerged the idea of the hardwall model,

which meant that a hard cutoff was introduced at a certain value z_{max} of the holographic coordinate z and it was considered a slice of AdS_5 space in the region $0 \leq z \leq z_{max}$.

Another holographic model to break the conformal invariance in the boundary theory, and make it an effective theory of QCD, is called the softwall model (SWM). This model introduces an exponential factor in the action related to a dilatonic field that represents a soft IR cutoff. The SWM was proposed in [25] to study vector mesons, and subsequently extended to glueballs [15]. One interesting property of the SWM is to provide linear Regge trajectories. In the ref. [23] it was shown that SWM does not work properly for calculation of scalar glueball and its radial excitation masses or higher spin glueball states. Due to this, one cannot find satisfactory Regge trajectories for glueballs from the SWM consistent with the literature.

In this work, our principal aim is to calculate Regge trajectories for both even and odd higher spin glueballs using a dynamical version of the SWM, i.e, imposing that the dilaton field became dynamical satisfying the Einstein equations in five dimensions [18]. The Regge trajectories obtained for both even and odd spin glueballs, related to the pomeron and the odderon, respectively, are in good agreement with available data.

II. THE DYNAMICAL HOLOGRAPHIC MODEL

The holographic dynamical softwall (DSW) model that we are going to consider has a metric structure which is consistently solved from Einstein's equation. To obtain the metric solution we write a 5D action for the graviton-dilaton coupling in the string frame:

$$S = \frac{G_5^{-1}}{16\pi} \int d^5x \sqrt{-g_s} e^{-2\Phi(z)} (\mathcal{R}_s + 4\partial_M \Phi \partial^M \Phi - V_G^s(\Phi)) \quad (1)$$

where G_5 is the Newton's constant in five dimensions, the dilaton field Φ is given by $\Phi = kz^2$, where $k \sim \Lambda_{QCD}^2$ and V_G is the dilatonic potential. The metric tensor in 5-dimensional space has the following form $g_{mn}^s = b_s^2(z)(dz^2 + \eta_{\mu\nu}dx^\mu dx^\nu)$ with $0 \leq z \leq \infty$, $m, n = 0, 1, 2, 3, 4$, $\mu, \nu = 0, 1, 2, 3$ and $\eta_{\mu\nu} = \text{diag}(-1, 1, 1, 1)$ and $b_s(z) \equiv e^{A_s(z)}$. All of these parameters are in the string frame. The precise form of the metric will be defined solving the equations of motion and finding explicitly the expression for $A_s(z)$. Actually, it is easier to solve this problem in the Einstein frame.

Performing a Weyl rescaling, from the string frame to the Einstein frame, such that

$b_E(z) = b_s(z)e^{-\frac{2}{3}\Phi(z)} = e^{A_E(z)}$ and $A_E(z) = A_s(z) - \frac{2}{3}\Phi(z)$, one can rewrite the action (1) as:

$$S = \frac{G_5^{-1}}{16\pi} \int d^5x \sqrt{-g_E} \left(\mathcal{R}_E - \frac{4}{3} \partial_m \Phi \partial^m \Phi - V_G^E(\Phi) \right) \quad (2)$$

where $g_{mn}^E = g_{mn}^s e^{-\frac{2}{3}\Phi}$ and $V_G^E = e^{\frac{4}{3}\Phi} V_G^s$. Varying this action, one can obtain the equations of motion:

$$-A_E'' + A_E'^2 - \frac{4}{9}\Phi'^2 = 0; \quad (3)$$

$$\Phi'' + 3A_E'\Phi' - \frac{3}{8}e^{2A_E}\partial_\Phi V_G^E(\Phi) = 0. \quad (4)$$

Solving these equations for the quadratic dilaton $\Phi = kz^2$, one finds:

$$A_E(z) = \log\left(\frac{R}{z}\right) - \log({}_0F_1(5/4, \frac{\Phi^2}{9})); \quad (5)$$

$$V_G^E(\Phi) = -\frac{12}{R^2} {}_0F_1(1/4, \Phi^2/9)^2 + \frac{16}{3R^2} {}_0F_1(5/4, \Phi^2/9)^2 \Phi^2, \quad (6)$$

where R is the AdS radius.

Going back to string frame, one can write the $5D$ action for the scalar glueball as [15]:

$$S = \int d^5x \sqrt{-g_s} \frac{1}{2} e^{-\Phi(z)} [\partial_M \mathcal{G} \partial^M \mathcal{G} + M_5^2 \mathcal{G}^2] \quad (7)$$

and the equations of motion are:

$$\partial_M [\sqrt{-g_s} e^{-\Phi(z)} g^{MN} \partial_N \mathcal{G}] - \sqrt{-g_s} e^{-\Phi(z)} M_5^2 \mathcal{G} = 0. \quad (8)$$

Representing the scalar field through a $4d$ Fourier transform $\tilde{\mathcal{G}}(q, z)$ and performing a change of function $\tilde{\mathcal{G}} = \psi(z)e^{\frac{B(z)}{2}}$, where $B(z) = \Phi(z) - 3A_s(z)$, one gets the following $1d$ Schrödinger-like equation

$$-\psi''(z) + V(z)\psi(z) = (-q^2)\psi(z), \quad (9)$$

where the effective potential is given by

$$V(z) = k^2 z^2 + \frac{15}{4z^2} - 2k + \left(\frac{M_5 R}{z}\right)^2 e^{4kz^2/3} \mathcal{A}^{-2}, \quad (10)$$

with $\mathcal{A} = {}_0F_1(5/4, \frac{\Phi^2}{9})$. The normalizable solutions of Eq. (9) correspond to a discrete spectrum of $4d$ masses with the identification $q^2 = -m_n^2$. This equation was solved numerically

in [18] for the scalar glueball 0^{++} and its radial (spin 0) excitations and the masses found are compatible with those from lattice QCD.

From the AdS/CFT dictionary one knows how to relate the operator in the super Yang-Mills theory with fields in the $AdS_5 \times S^5$ space. In the case of dual higher spin fields we consider a symmetric traceless spin J field and the relation between the conformal dimension Δ and the AdS mass is

$$M_5^2 R^2 = \Delta(\Delta - 4) - J; \quad (J = 0, 1, 2, 3, \dots) \quad (11)$$

and the effective potential reads

$$V_J(z) = k^2 z^2 + \frac{15}{4z^2} - 2k + \frac{\Delta(\Delta - 4) - J}{z^2} e^{4kz^2/3} \mathcal{A}^{-2}. \quad (12)$$

III. EVEN SPINS AND THE POMERON.

In the perturbative approach, the pomeron is identified with the leading twist 2 trajectory $\Delta = J + 2$ (see, e. g., [14] and refs. therein). Note that for twist two operator the relation (11) gives $M^2 = J^2 - J - 4$ as shown in [25]. So, let us start this study with this assumption. Using the DSW model discussed in the previous section, one obtains complex masses for the glueball states 0^{++} and 2^{++} which does not allow us to find a Regge trajectory for the pomeron. However, in the non-perturbative regime higher twist operators also contribute to the scattering amplitudes related to the pomeron [26]. Furthermore, in ref. [27] it was argued that the glueball state 0^{++} does not belong to the pomeron trajectory, but to another one with lower intercept. This does not agree with [26] where the 0^{++} state is taken into account to the pomeron trajectory. In order to investigate these problems, we are going to consider trajectories including and excluding the 0^{++} state and with higher twist.

So now we consider twist four operators for a pure super Yang-Mills theory defined on the 4D boundary, such that $\Delta = J + 4$ and compute the masses for even glueball states using eqs. (11) and (12). The scalar glueball state 0^{++} is represented by the operator \mathcal{O}_4 , and it can be written as $\mathcal{O}_4 = Tr(F^2) = Tr(F^{\mu\nu} F_{\mu\nu})$. For higher spin glueballs we insert symmetrized covariant derivatives in a given operator with spin in order to raise the total angular momentum. Then, one obtains $\mathcal{O}_{4+J} = F D_{\{\mu 1 \dots D_{\mu J\}} F$, with conformal dimension $\Delta = 4 + J$ and spin J .

To calculate the masses for the higher spin glueball states and get the Regge trajectory related to the pomeron, one has to solve the eq. (9) numerically with the effective potential (12). The masses found are shown in Table I.

	Glueball States J^{PC}						k
	0^{++}	2^{++}	4^{++}	6^{++}	8^{++}	10^{++}	
m_n	0.51	2.03	3.23	4.40	5.56	6.71	0.10

Table I: Masses m_n expressed in GeV for the glueball states J^{PC} with even J as the eigenstates of Eq. (9) with the potential (12) for $k = 0.10 \text{ GeV}^2$.

Regge trajectories are an approximate linear relation between total angular momenta (J) and the square of the masses (m), such that $J(m^2) \approx \alpha_0 + \alpha' m^2$ with α_0 and α' constants. One can obtain Regge trajectories for the pomeron using data from Table I once they are associated with even spin glueballs.

For instance, a Regge trajectory can be obtained from eq.(9) for the pomeron using table I and $k = 0.10 \text{ GeV}^2$, excluding the state 10^{++} , and is presented below:

$$J(m^2) \approx (0.72 \pm 0.49) + (0.25 \pm 0.02)m^2 \quad (13)$$

The errors come from the linear fit. This Regge trajectory for the pomeron is represented in Figure 1 (left panel) and is in agreement with the one presented in [28].

Choosing another set of states, for example, $2^{++}, 4^{++}, 6^{++}$, from Table I also with $k = 0.10 \text{ GeV}^2$, one finds the following Regge trajectory:

$$J(m^2) = (1.06 \pm 0.33) + (0.26 \pm 0.02)m^2 \quad (14)$$

which is represented in Figure 1 (right panel) and is in excellent agreement with [28] and also with [27] where the state 0^{++} was excluded.

We plot in Figure 2 (left panel) the shape of the effective potential $V_J(z)$ in the DSW model for different values of the spin J . One can see that in the UV limit ($z \rightarrow 0$) all plots have a similar behavior. But in the IR region ($z \rightarrow \infty$) they differ clearly for different spins. The higher the spin of the glueball, the higher is the slope of the effective potential at large z . Also the minimum of the potential increases with the spin of the glueball.

For comparison, we show in Figure 2 (right panel) the corresponding effective potentials for the SWM extended for high spins [23]. These effective potentials also increase fast for

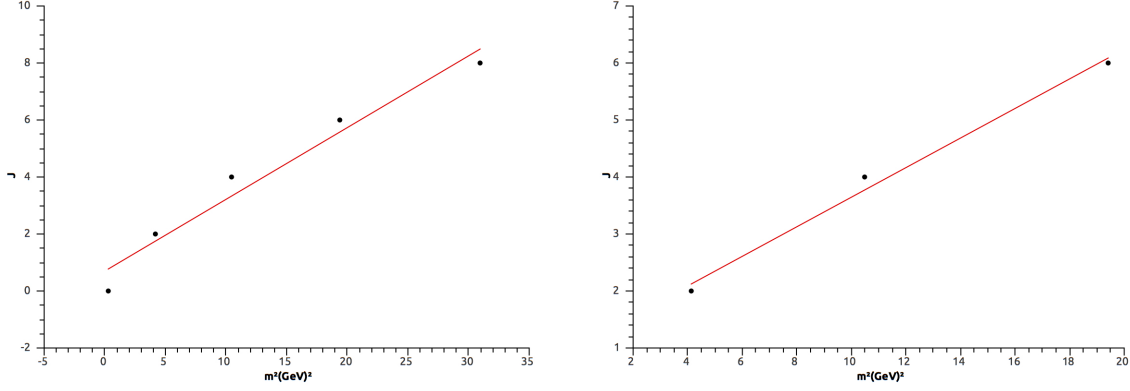


Figure 1: Regge trajectories for the pomeron, from data of Table I with $k = 0.1 \text{ GeV}^2$. Left panel: glueball states $0^{++}, 2^{++}, 4^{++}, 6^{++}$, and 8^{++} and trajectory given by eq. (13). Right panel: glueball states $2^{++}, 4^{++}$ and 6^{++} and trajectory given by eq. (14).

small z , but they increase slowly for large z , in contrast with the holographic dynamical model shown in Figure 2 (left panel).

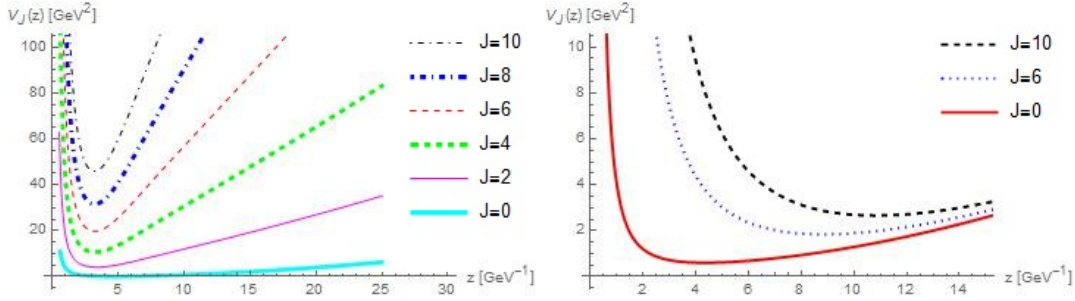


Figure 2: Plots of the effective potentials $V_J(z)$ against the holographic coordinate z for some values of even spins. Left panel: $J = 0, 2, \dots, 10$ and effective potential given by Eq. (12), in the DSW model. Right panel: $J = 0, J = 6$, and $J = 10$ in the SWM.

IV. ODD SPINS AND THE ODDERON.

For odd spin glueballs, the operator \mathcal{O}_6 that describes the glueball state 1^{--} is given by $\mathcal{O}_6 = \text{SymTr} \left(\tilde{F}_{\mu\nu} F^2 \right)$ and after the insertion of symmetrized covariant derivatives one obtains $\mathcal{O}_{6+J} = \text{SymTr} \left(\tilde{F}_{\mu\nu} F D_{\{\mu 1 \dots D_{\mu J\}} F \right)$, with conformal dimension $\Delta = 6 + J$ and spin $1 + J$.

To calculate the masses for the higher spin glueball states and get the Regge trajectory

related to the odderon, we solve the eq. (9) with the effective potential (12) numerically for odd J . The masses eigenstates found for odd glueball states are shown in Table II.

	Glueball States J^{PC}						k
	1^{--}	3^{--}	5^{--}	7^{--}	9^{--}	11^{--}	
m_n	2.77	3.91	5.05	6.19	7.33	8.47	0.10

Table II: Masses m_n expressed in GeV for the glueball states J^{PC} with odd J solving Eq. (9) with the potential (12) for $k = 0.10 \text{ GeV}^2$.

Regge trajectories for the odderon can be obtained using data from Table II since they are associated with odd spin glueballs.

For the odderon, using table II and $k = 0.10 \text{ GeV}^2$, excluding the state 11^{--} , the Regge trajectory is presented bellow:

$$J(m^2) \approx (0.20 \pm 0.43) + (0.17 \pm 0.01)m^2 \quad (15)$$

The errors come from the linear fit. This Regge trajectory for the odderon is represented in Figure 3 (left panel) and is in agreement with [29] within the non-relativistic constituent model.

Choosing another set of states, for exemple, $1^{--}, 3^{--}, 5^{--}$, from Table II also with $k = 0.10 \text{ GeV}^2$, one finds the following Regge trajectory:

$$J(m^2) = (-0.60 \pm 0.33) + (0.22 \pm 0.01)m^2 \quad (16)$$

which is compatible with [29] within the relativistic many-body model. This Regge trajectory for the odderon is represented in Figure 3 (right panel) and the errors also come from the linear fit.

Another set with $3^{--}, 5^{--}, 7^{--}$, from Table II also with $k = 0.10 \text{ GeV}^2$ gives

$$J(m^2) = (0.44 \pm 0.32) + (0.17 \pm 0.01)m^2 \quad (17)$$

which is compatible with the non-relativistic constituent model [29] and excludes the state 1^{--} .

Figure 4 (left panel) represents the effective potentials in the DSW model for various odd spin glueball states. For comparison, we show in Figure 4 (right panel) the corresponding

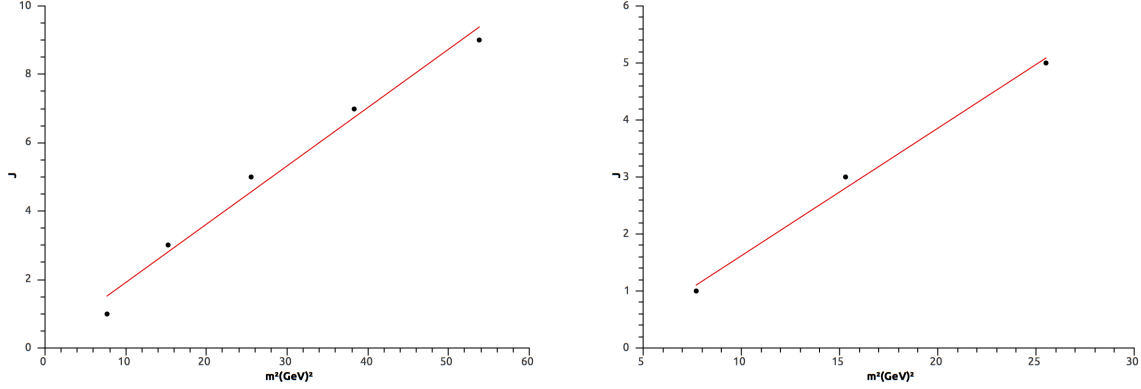


Figure 3: Regge trajectories for the odderon, from data of Table II with $k = 0.1 \text{ GeV}^2$. Left panel: glueball states $1^{--}, 3^{--}, 5^{--}, 7^{--}, 9^{--}$ and trajectory given by eq. (15). Right panel: glueball states $1^{--}, 3^{--}, 5^{--}$ and trajectory given by eq. (16).

effective potentials for the usual SWM extended for high spins [23]. These effective potentials also increase fast for small z , but they increase slowly for large z , in contrast with the holographic dynamical model shown in Figure 4 (left panel).

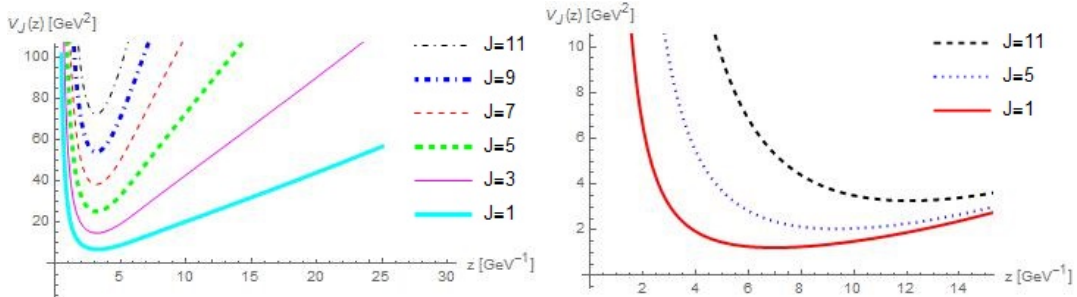


Figure 4: Plots of the effective potentials $V_J(z)$ against the holographic coordinate z for some values of odd spins. Left panel: $J = 1, 3, \dots, 11$ and effective potential given by Eq. (12), in the DSW model. Right panel: $J = 1, J = 5$, and $J = 11$ in the SWM.

V. CONCLUSIONS

We used a dynamical holographic softwall model to obtain even and odd spin glueball mass spectra and achieve the related Regge trajectories associated with the pomeron and the odderon, respectively. These trajectories are in good agreement with those found in [13, 17, 22, 23, 27–29]. Besides, this is the first obtention of these Regge trajectories through

a dynamical model.

In particular, it has been shown in [23] that the SWM could not lead to the expected Regge trajectories for the pomeron or the odderon. This problem is overcome in this work by the use of the DSW model.

The masses obtained in this work can be compared with the ones coming from some phenomenological models. First, the masses found here from the DSW model are higher than those found from the SWM [23], if one chooses the same value of the free parameter k . This fact can be understood comparing the plots $V_J(z) \times z$ for these two models. Figures 2 and 4 (both left panels) represent the effective potential for the DSW model for some even and odd spin glueball states while Figures 2 and 4 (both right panels) represent the corresponding potentials for the softwall model. Since the minima of the effective potentials for the DSW model are higher than those of the SWM, the corresponding masses eigenstates for the DSW model are higher than those from the SWM.

Second, the masses found from the DSW model are similar to those found in refs. [13, 17] within the holographic hardwall model [30]. This fact can be understood also comparing Figures 2 and 4 (left panels) for the DSW model with Figures 2 and 4 (right panels) for the SWM. One can see that in Figures 2 and 4 (left panels) the effective potentials increase with larger slopes for each spin than those in Figures 2 and 4 (right panels). This means that the dynamical corrections of the SWM produce barriers for the effective potential similar to those of the phenomenological hardwall model.

In ref. [27] it was argued that the state 0^{++} does not belong to the pomeron's Regge trajectory. Our results on the Regge trajectories for the pomeron, showed in Eqs. (13) and (14) are not conclusive in this regard. In Eq. (13) we obtain a Regge trajectory for the pomeron including the state 0^{++} which is in agreement with [28] and [22]. On the other side, in Eq. (14) we obtain a Regge trajectory for the pomeron excluding the state 0^{++} which is also compatible with experimental data [28]. Note, however, that this is our best fit for the pomeron trajectory.

In the case of the odderon, different Regge trajectories were found in [29] corresponding to a relativistic and a non-relativistic models. We found compatible results within the DSW model for both the relativistic and non-relativistic predictions for the odderon as presented in [29]. Also, in ref. [29] it was argued that the state 1^{--} should not belong to the odderon Regge trajectory. This conclusion is not supported by our results with the DSW model for

the exclusion of the 1^{--} state, since we found good trajectories for the odderon with and without the glueball state 1^{--} .

Acknowledgments

H.B.-F. is partially supported by CNPq and E.F.C. by CNPq and FAPERJ, Brazilian agencies. D.L. is supported by the China Postdoctoral Science Foundation.

-
- [1] C. F. Qiao and L. Tang, Phys. Rev. Lett. **113**, no. 22, 221601 (2014) [arXiv:1408.3995 [hep-ph]].
 - [2] A. Chuinard, C. Royon and R. Staszewski, arXiv:1510.04218 [hep-ph].
 - [3] J. M. Maldacena, Adv. Theor. Math. Phys. **2**, 231 (1998) [hep-th/9711200].
 - [4] S. S. Gubser, I. R. Klebanov and A. M. Polyakov, Phys. Lett. B **428**, 105 (1998) [hep-th/9802109].
 - [5] E. Witten, Adv. Theor. Math. Phys. **2**, 253 (1998) [hep-th/9802150].
 - [6] E. Witten, Adv. Theor. Math. Phys. **2**, 505 (1998) [hep-th/9803131].
 - [7] O. Aharony, S. S. Gubser, J. M. Maldacena, H. Ooguri and Y. Oz, Phys. Rept. **323**, 183 (2000) [hep-th/9905111].
 - [8] J. Polchinski and M. J. Strassler, Phys. Rev. Lett. **88**, 031601 (2002) [hep-th/0109174].
 - [9] J. Polchinski and M. J. Strassler, JHEP **0305**, 012 (2003) [hep-th/0209211].
 - [10] H. Boschi-Filho and N. R. F. Braga, JHEP **0305**, 009 (2003) [hep-th/0212207].
 - [11] H. Boschi-Filho and N. R. F. Braga, Eur. Phys. J. C **32**, 529 (2004) [hep-th/0209080].
 - [12] G. F. de Teramond and S. J. Brodsky, Phys. Rev. Lett. **94**, 201601 (2005) [hep-th/0501022].
 - [13] H. Boschi-Filho, N. R. F. Braga and H. L. Carrion, Phys. Rev. D **73**, 047901 (2006) [hep-th/0507063].
 - [14] R. C. Brower, J. Polchinski, M. J. Strassler and C. I. Tan, JHEP **0712**, 005 (2007) [hep-th/0603115].
 - [15] P. Colangelo, F. De Fazio, F. Jugeau and S. Nicotri, Phys. Lett. B **652** (2007) 73 [hep-ph/0703316].
 - [16] R. C. Brower, M. Djuric and C. I. Tan, JHEP **0907**, 063 (2009) [arXiv:0812.0354 [hep-th]].

- [17] E. F. Capossoli and H. Boschi-Filho, Phys. Rev. D **88**, no. 2, 026010 (2013) [arXiv:1301.4457 [hep-th]].
- [18] D. Li and M. Huang, JHEP **1311**, 088 (2013) [arXiv:1303.6929 [hep-ph]].
- [19] R. C. Brower, M. S. Costa, M. Djurić, T. Raben and C. I. Tan, JHEP **1502**, 104 (2015) [arXiv:1409.2730 [hep-th]].
- [20] F. Brünner and A. Rebhan, Phys. Rev. Lett. **115**, no. 13, 131601 (2015) [arXiv:1504.05815 [hep-ph]].
- [21] L. Bellantuono, P. Colangelo and F. Giannuzzi, JHEP **1510**, 137 (2015) [arXiv:1507.07768 [hep-ph]].
- [22] A. Ballon-Bayona, R. Carcasses Quevedo, M. S. Costa and M. Djuric, Phys. Rev. D **93**, 035005 (2016) [arXiv:1508.00008 [hep-ph]].
- [23] E. F. Capossoli and H. Boschi-Filho, Phys. Lett. B **753** (2016) 419 [arXiv:1510.03372 [hep-ph]].
- [24] Y. Chen and M. Huang, arXiv:1511.07018 [hep-ph].
- [25] A. Karch, E. Katz, D. T. Son and M. A. Stephanov, Phys. Rev. D **74**, 015005 (2006) [hep-ph/0602229].
- [26] S. Donnachie, H. G. Dosch, O. Nachtmann and P. Landshoff, “Pomeron physics and QCD,” Camb. Monogr. Part. Phys. Nucl. Phys. Cosmol. **19**, 1 (2002).
- [27] H. B. Meyer and M. J. Teper, Phys. Lett. B **605**, 344 (2005) [hep-ph/0409183].
- [28] P. V. Landshoff, hep-ph/0108156.
- [29] F. J. Llanes-Estrada, P. Bicudo and S. R. Cotanch, Phys. Rev. Lett. **96**, 081601 (2006) [hep-ph/0507205].
- [30] This identification works better for the hardwall model with Neumann boundary condition, which has good agreement with experimental data.